

Solar PV System with Battery Energy Storage for Critical Load

Shridhar S. Khule, Sharad W. Mohod

Abstract — In a microgrid network, it is difficult to supply the critical load without energy storage, especially when renewable energy sources are used. The proposed solar PV system with battery energy storage is used to supply the controllable real and non-active power to the load. The generated solar power can be extracted under varying irradiance and temperature condition and can be stored in the batteries at low power demand hours. In proposed scheme, inverter control is implemented with active and non-active power control mode to achieve the faster dynamic switchover for the support of critical load. The Battery storage appended with solar PV system synthesizes the output waveform by injecting or absorbing non-active power and enable the real power flow required by the load. The system reduces the burden on the conventional source and utilizes solar PV to supply critical load constraints. Thus, the system provides fast response to support the critical loads. The scheme can also be operated in an islanded mode in case of grid failure. MATLAB/SIMULINK software is used to simulate the proposed system and results are presented.

Keywords— Microgrid, solar PV Generator, battery energy storage, critical load.

I. INTRODUCTION

With high population growth and economic development in the world, there is a very high demand for energy. Traditional fossil fuel based power networks are facing confrontation due to the emerging crisis of these non sustainable resources, poor energy efficiency and increased environmental pollution. As a renewable energy, solar energy generation has been focused as a clean and inexhaustible energy providing a feasible solution to energy shortage [1]-[5]. The microgrid consisting of solar PV system with battery back-up is becoming more prominent with the increasing demand of power generation [6]. It increases the reliability of the system with reduced environment pollution. However the sporadic nature of solar PV source causes fluctuation in output power and will affect the operation in the distribution network. The residential, industrial and commercial consumers often operate the sensitive electronic equipments or critical load that cannot tolerate voltage deviation or loss of power, which moreover cause decrease in life of operating equipments or stoppage in industrial production [7]. Therefore there is a pressing need to mitigate the output fluctuation so as to supply quality power to the loads. The battery storage appended with solar PV system can provide the effective, reliable solution to the distributed power system. However, to maintain the voltage and frequency within permissible limit, the operation and control

of the inverter interface of solar PV in a microgrid is a real challenge [8]. Researchers in [9] proposed a voltage control method based on traditional droop control for voltage sag mitigation. Frequency regulation of a microgrid using solar power is explained in [10], however the battery storage is not considered. The coordinated control of solar PV system with battery back-up in microgrid is investigated in [11]; however this work lacks consideration of battery SOC constraint. In summary, the previous work either lack consideration of battery storage or incorporation of control transition in different scenarios. The proposed control strategy with battery storage fulfills these gaps by considering following objectives.

- To supply real and non-active power from solar PV system and battery to the load
- To extricate maximum power from solar PV generator
- To maintain State of Charge (SOC) of battery
- Stand-alone operation of microgrid

The rest of the paper is organized as follows. Section II introduces the proposed microgrid. Section III briefly presents solar energy extraction with batteries. Section IV describes proposed active-reactive power (P-Q) control and battery SOC control strategies. Section V discusses experimental results. Section VI finally draws the conclusions.

II. PROPOSED MICROGRID

A microgrid architecture consisting of solar PV generator, battery energy storage, Diesel Generator (D-G) set and load is illustrated in Fig. 1. The microgrid consists of renewable energy resources, which are small units provided with power electronics (PE) interface. To obtain the maximum power under varying operating conditions, the solar PV array is integrated through a DC-DC boost converter and controlled using a Maximum Power Point Tracking (MPPT) algorithm [12]. The solar PV array is integrated through a DC-DC boost converter and controlled using a Maximum Power Point Tracking (MPPT) algorithm to obtain the maximum power under varying operating conditions [12]. The Battery Energy Storage System (BESS) is concatenated through buck boost converter to maintain state of charge of battery. BESS offers charging during the daytime when the irradiance is large and load is less, and discharging when the irradiance is less and load is more. The converter is used either in buck or boost mode to charge or discharge the battery respectively. The control signal provided to the converter switches maintains the operation mode.

Revised Manuscript Received on December 22, 2018.

Shridhar S. Khule, Research Scholar, Prof. Ram Meghe Institute of Technology and Research, Badnera, Amravati, Maharashtra, India

Sharad W. Mohod, Professor, Prof. Ram Meghe Institute of Technology and Research, Badnera, Amravati, Maharashtra, India



Solar PV System with Battery Energy Storage for Critical Load

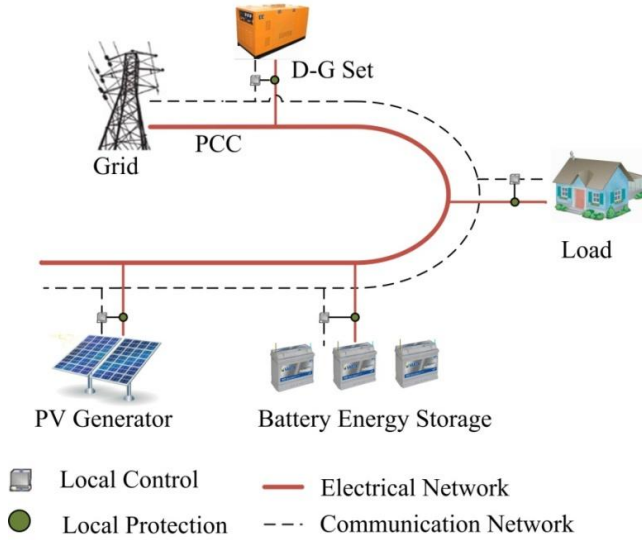


Fig.1. Microgrid Architecture

The D-G set is used to maintain power balance within the system. To maintain the system frequency within permissible limit under varying generation and loads, D-G set is used. The inductor L_c couples the solar PV system to the microgrid. The coupling inductor makes the PV output current ripple free. The PV is the active power source, and the capacitor is the reactive power source.

TABLE 1. MICROGRID SYSTEM PARAMETERS

Description	Values
Point of Common Coupling	3-phase, 415 V, 50 Hz
Solar PV System	100 kW
Battery	Cell capacity 300Ah, Type-Lead acid
Interfacing transformer	120kVA, 440/480 V, Y-Δ, 50 Hz
Diesel Generator	150 kVA, 415 V, 50 Hz
Load	3-phase, 170 kW

III. SOLAR ENERGY EXTRACTION WITH BATTERIES

A. Solar PV Generator

Fig. 2 shows the equivalent circuit of the ideal PV cell. Equation (1) illustrates the I-V characteristics model of the ideal PV cell [13].

$$I = I_{pv,cell} - I_{0,cell} \left[\exp \left(\frac{q \cdot V}{\alpha \cdot k \cdot T} \right) - 1 \right] \quad (1)$$

where $I_{pv,cell}$ is the current generated by the incident light, I_d is the shockley diode equation, $I_{0,cell}$ is the diode's reverse saturation current, q is the electron charge ($1.60217646 \times 10^{-19}$), k is the Boltzmann constant ($1.3806503 \times 10^{-23}$ J/K), T is the p-n junction temperature in Kelvin, and α is the diode ideality constant.

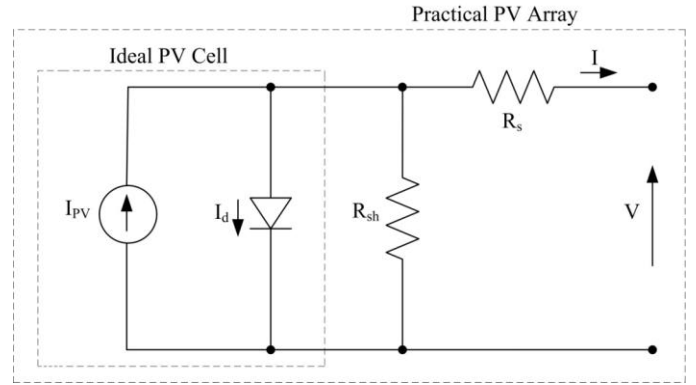


Fig.2. One diode model of ideal PV cell and equivalent circuit of practical PV array

The equivalent circuit of practical PV array is illustrated in Figure 2. Practical PV array consist of several series parallel combination of PV cells. The equation (2) represents I-V characteristics of practical PV array [13],

$$I = I_{PV} - I_0 \left[\exp \left(\frac{V + I R_s}{a V_{therm}} \right) - 1 \right] - \frac{V + I R_s}{R_{sh}} \quad (2)$$

Where I_{PV} is the photo current, I_0 is the diode saturation current, $V_{therm} = N_s k T / q$ is the thermal voltage of the array, N_s is the series connected cells, R_s and R_{sh} are the series and shunt resistances of the array, respectively. If the array consists of N_p parallel connected cells, the PV and saturation current can be modeled as $I_{pv} = I_{pv,cell} \cdot N_p$ and $I_0 = I_{0,cell} \cdot N_p$. The photocurrent of the PV array is a linear function of solar irradiance and the cell temperature as given in equation (3) [13].

$$I_{PV} = (I_{PV,n} + K_1 \Delta T) \frac{G}{G_n} \quad (3)$$

Where, $I_{PV,n} = \frac{R_{sh} + R_s}{R_{sh}} I_{sc}$ is the photocurrent at 25°C and

1000W/m², K_1 is the short circuit current / temperature coefficient, ΔT is the difference between the actual and nominal temperature in Kelvin; G is the irradiation on the device surface in W/m², and G_n is the nominal radiation in W/m².

These basic equations and physical parameters, derived from datasheet, are being employed to develop the PV model. The I-V characteristics for changing cell temperature at constant irradiance of 1000 W/m² are obtained and depicted in Fig. 3(a) and (b). Fig. 4(a) and (b) illustrates the changing irradiance at constant cell temperature of 25°C.

PV array composed of 20 parallel strings and each string having 25 series connected modules. In this work Kyocera Solar KC200GT model is used. The Maximum Power Point (MPP) for a single module at 1000 W/m² and 25°C (STC) is 200.143 W. Hence the maximum power of solar PV array at STC is $20 \times 25 \times 200.143 = 100.071$ kW.

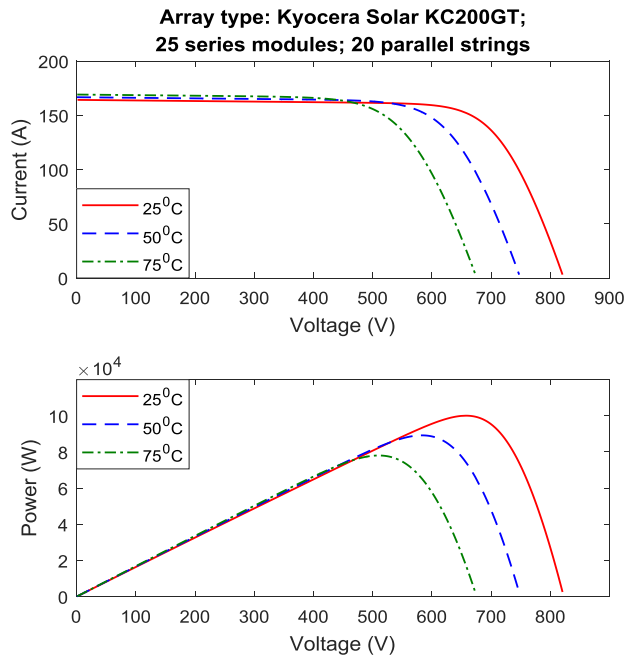


Fig. 3. PV array (a) I-V and; (b) P-V characteristic with varying cell temperature at 1000 W/m² irradiance

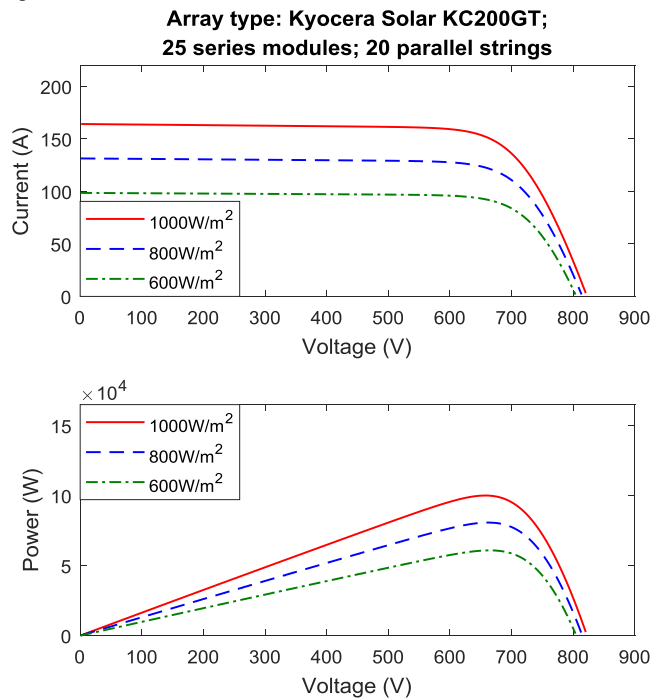


Figure 4: PV array (a) I-V and; (b) P-V characteristic with varying irradiance at a cell temperature of 25°C

B. Dc link for battery storage and solar PV generator

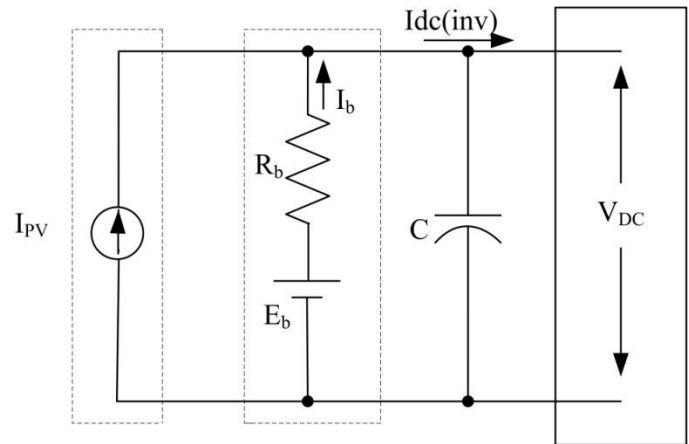


Fig. 5. DC link for solar PV generator and battery storage

The battery storage and Solar PV are connected across the dc link is illustrated in Fig. 5. The dc link consists of capacitor which dissociate the PV system and ac source (grid) system [7], [14]. Due to sporadic nature of solar power output and the fluctuations in load, energy storage is generally needed in microgrid applications. The deep cycle lead acid batteries are the most common type of battery storage in microgrid because maximum charge of the battery can be utilized. Hence in this paper lead acid battery model [15] is used. The use of capacitor in dc link is efficient as well as cost effective and is modeled as follows:

$$C \frac{d}{dt} V_{dc} = I_{pv} - I_{dc(inv)} - I_b \quad (4)$$

Where C is dc link capacitance, V_{dc} is terminal voltage, I_{pv} is PV current, $I_{dc(inv)}$ is inverter dc-side current, and I_b is the battery current.

The battery storage is cascaded to dc link and is represented by a voltage source E_b connected in series with an internal resistance R_b . The internal voltage varies with the charged state of the battery. The terminal voltage V_{dc} is given by (5).

$$V_{dc} = E_b - I_b * R_b \quad (5)$$

Where, I_b is the battery current.

It is necessary to keep adequate dc link level to meet the inverter voltage given in (6).

$$V_{dc} \geq \frac{\sqrt{3}}{M_a} V_{inv} \quad (6)$$

where V_{inv} is the line-to-neutral rms voltage of inverter (240 V_{rms}), inverter output frequency 50 Hz, and M_a is modulation index [16]. Therefore, the dc link is designed for 700 V.

CONTROL SCHEME OF THE SYSTEM

The control scheme with solar PV generator and battery storage utilizes the dc link to extract the energy from the solar. The dual combination of solar PV generator and battery storage is connected through three leg inverter to the distribution system. The battery facilitates to maintain the dc bus voltage constant. The schematic is depicted in Fig. 6.

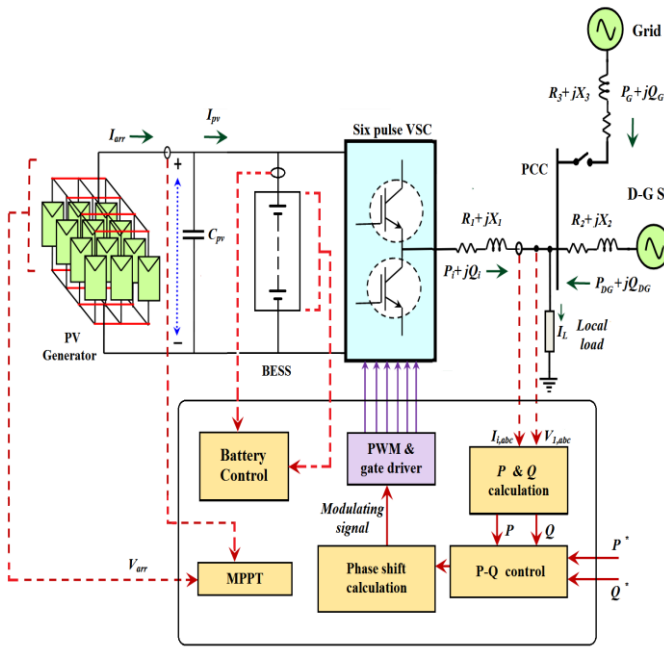


Fig. 6. Schematic of control strategy

The MPPT controller is used to track maximum power point. Reference Maximum Power Point (MPP) is obtained from look up table of irradiance versus MPP. Measured Solar PV output power is compared with this reference MPP power to generate error for PI₁ controller. This controller gives the duty cycle output for the DC-DC converter to ensure that PV array will always operates at the reference MPP point. The duty cycle is given by [17-18].

$$\delta^* = K_{p1}(P_{MPPref} - P_{PVActual}) + K_{I1} \int_0^t (P_{MPPref} - P_{PVActual}) dt \quad (7)$$

where, K_{p1} is controller proportional gain and K_{I1} controller integral gains respectively.

The active power can be controlled by controlling the inverter side real output power. The actual measured active power is compared with reference active power and then error is given to PI₂ controller which will give the phase shift α_1^* . This phase shift is given by [17-18].

$$\alpha_1^* = K_{p2}(P_{ref} - P_{actual}) + K_{I2} \int_0^t (P_{ref} - P_{actual}) dt \quad (8)$$

To keep the real power balance at DC and AC side of inverter, PI₃ controller is used. The AC side measured real power is multiplied by a factor of 1.02 considering efficiency of inverter as 98%. The DC real power is compared with this value of AC power and then error is given to PI₃ controller which will give the phase shift α_2^* . This phase shift is given by [17-18].

$$\alpha_2^* = K_{p3}(1.02 * P_{ACmeasured} - P_{DC}) + K_{I3} \int_0^t (1.02 * P_{ACmeasured} - P_{DC}) dt \quad (9)$$

The phase shift contributions from both sides of inverter are averaged which will obtain the final phase shift given by (10) and then it will generates the reference signal of voltage v_c^* for the inverter PWM.

$$\alpha^* = (\alpha_1^* + \alpha_2^*)/2 \quad (10)$$

The measured non-active power injection at PCC is compared with the reference non-active power and this error signal is passed to the PI controller, PI₄. Then, the output of PI₄ is multiplied by the terminal voltage v_t to obtain the reference voltage v_c^* which is in phase with v_t . The inverter output voltage is given by (11)

$$v_c^* = (K_{p2}(Q_{ref} - Q_{actual})) + K_{I2} \int_0^t (Q_{ref} - Q_{actual}) dt + v_t \quad (11)$$

The solar PV generator is supported by Battery Energy Storage (BES) for critical load application. When there is abundant solar power and solar PV output power at MPP (P_{pv}) is more than or equal to the active power required for controlling the frequency (Pinverter) i.e. $P_{pv} \geq P_{inverter}$, then the battery is in charging mode. If there is reduced solar insolation and the active power required to control the frequency (Pinverter) is more than the solar PV output power (P_{pv}) i.e. $P_{inverter} > P_{pv}$, then the battery is in discharging mode.

The average power of PV at PCC for a balanced three phase system is explained in [19]. The average power flow for the proposed system can be monitored on PCC for active and non-active power flow (P_{DG} , Q_{DG}) of the D-G set, Inverter power (P_i , Q_i) and the load (P_L , Q_L) is illustrated in Figure 7.

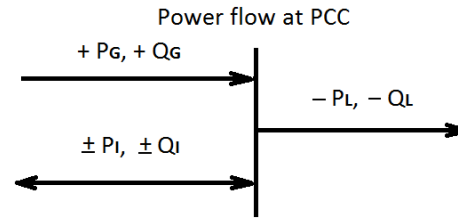


Fig. 7. Active and reactive power flow at PCC

RESULTS AND DISCUSSION

The microgrid is implemented in MATLAB environment to analyze the performance of the proposed control strategy. This system is tested under following conditions:

Switching frequency = 5 kHz;

Supply frequency = 50 Hz;

DC link voltage = 700 V;

Phase to neutral voltage = 240 V;

Critical load = 90 kW;

Filter inductor = 1 mH;

Filter capacitor = 0.5 μ F;

The Diesel-Generator (D-G) set is design to supply 150 kVA. Initially, the microgrid is connected to the utility grid. The grid is disconnected at $t = 4$ sec. Fig. 8 illustrates the electrical parameters at grid before and after grid connection. The D-G set is operated at $t = 4$ sec in the synchronous island mode. The active and non-active power supplied by the D-G set is shown in fig. 9. It supplies 75kW active and 70 kVAR non-active power to the load. Fig. 10 shows the reference active and non-active power of the inverter. The reference active and non-active power are 90 kW and 30 kVAR respectively. The reference values represents the critical

load of microgrid. To verify charging and discharging process of battery energy storage above reference values are selected. Fig. 11 shows the plot of active power from solar PV generator, inverter and active power to battery. In this case 1000 W/m^2 solar irradiance is considered. The power from solar PV at MPP is 100 kW . Here, reference critical active power demanded by load is less than the solar PV power, inverter supply 90 kW to the critical load and 8 kW to the battery. The negative power of battery indicates that it is being charged. Fig. 12 illustrates the voltage at PCC in p.u. Due to islanding of microgrid at $t = 4 \text{ sec}$, voltage suddenly drops to 0.87 p.u. and recovers within 0.9 sec . When islanding occurred at $t = 4 \text{ sec}$, the power supplied from main grid was cut, and frequency dropped to 48.9 Hz due generation load mismatch as shown in fig. 13. The State of Charge (SOC) of battery is shown in fig. 14. The battery control starts at $t = 2 \text{ sec}$. Since solar PV power exceeds the required critical power, surplus power is fed to charge the battery.

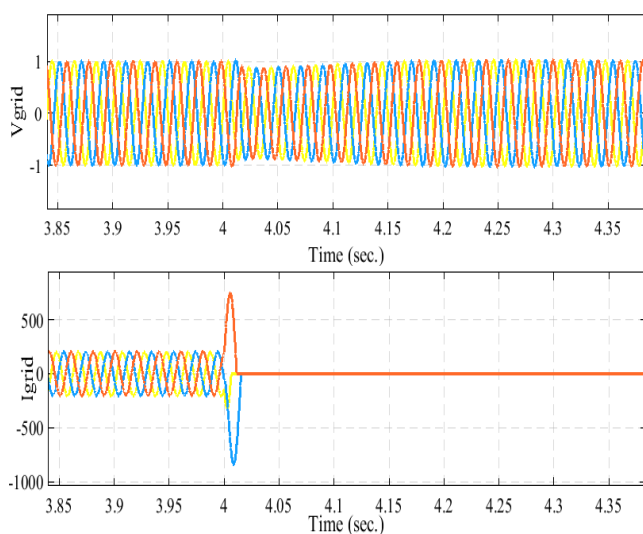


Fig. 8. From grid connected to intentional islanding operation

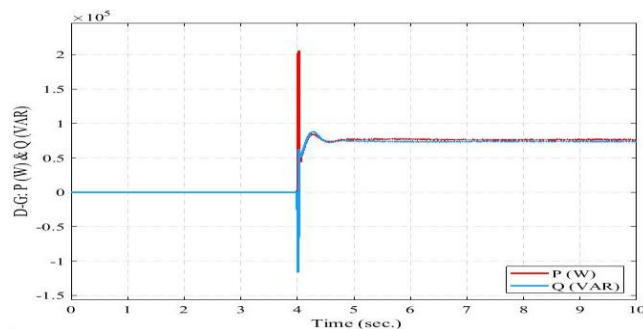


Fig. 9. D-G set active and reactive power

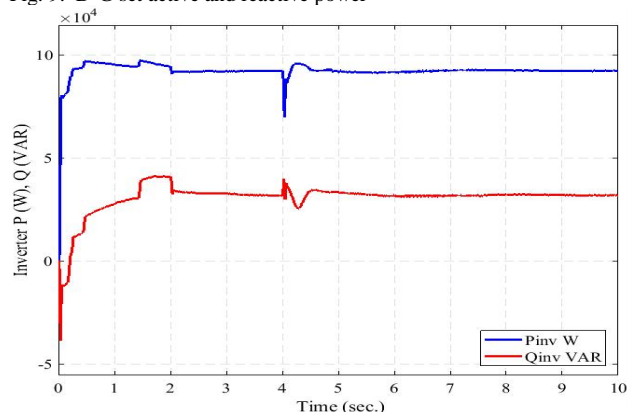


Fig. 10. Inverter active and reactive power

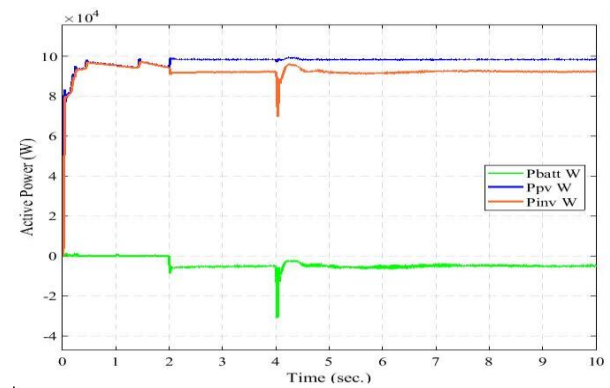


Fig. 11. PV, inverter and battery active power

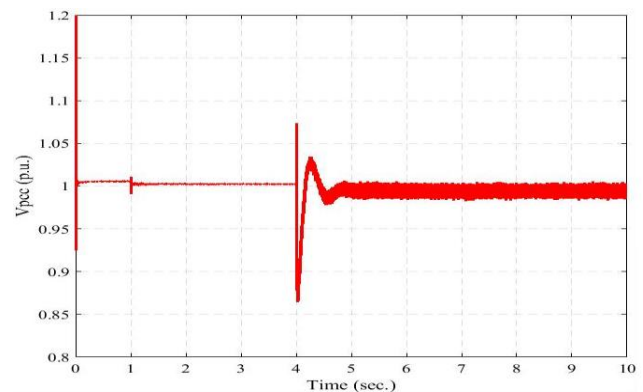


Fig. 12. Voltage at PCC

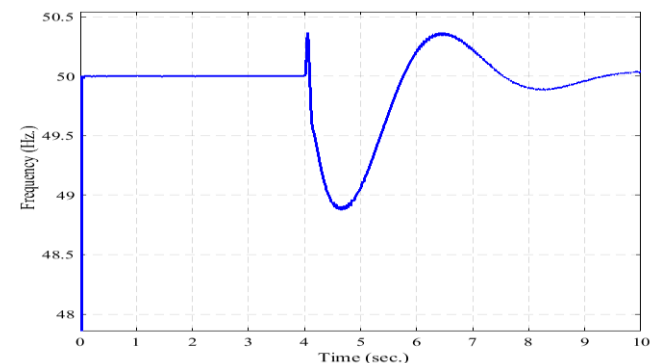


Fig. 13. Frequency at PCC

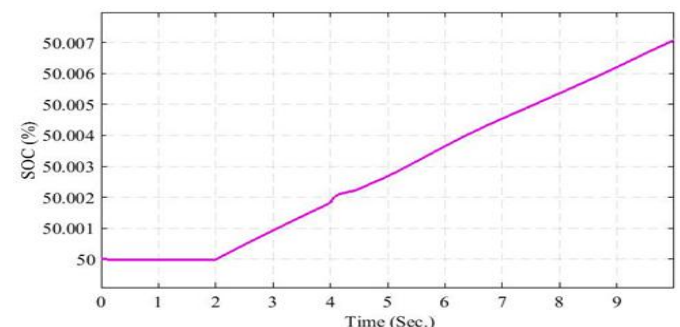


Fig. 14. State of Charge of battery

IV. CONCLUSION

This paper proposes coordinated voltage-frequency control strategy for sharing of power among Distributed Energy Resources in islanded microgrid. In this



control strategy MPPT is used to extricate maximum power from solar PV system, and battery storage is used as a buffer in order to store or supply deficit power by using the battery storage. The results clearly show that the battery control strategy handles SOC constraint of the battery. An effective smooth transition of control from voltage - control to constant active power control at the solar PV side and from constant active power control to frequency control at the D-G side is validated. This feature helps the controller to adapt with changing irradiance and battery availability. The proposed control method shows that the voltage and frequency quickly settles down to the reference values as compared to diesel generator control.

REFERENCES

1. S.W. Mohod, and M. V. Aware, "A STATCOM- Control Scheme for Grid Connected Wind Energy System for Power Quality Improvement," IEEE System Journal, Vol 4, No. 3, pp.346-352, 2010.
2. Magdi S. Mahmoud, Nezar M. Alyazidi, Mohamed I. Abouheaf, "Adaptive Intelligent Techniques for Microgrid Control Systems: A Survey," Electrical Power and Energy Systems 292–305, 2017.
3. Blaabjerg F, Teodorescu R, Liserre M, Timbus AV, "Overview of Control and Grid Synchronization for Distributed Power Generation System," IEEE Trans Ind Electro, pp.1398-409, 2006.
4. Mahmoud MS. Azher SH. Abido MA., "Modeling and Control of Microgrid: An Overview," J Franklin Ins, 351(5), 2822-59, 2014.
5. R. H. Lasseter, "MicroGrids," in Proc. IEEE Power Engineering Society Winter Meeting, Vol. 1, pp. 305–308, 2002.
6. Haihua Zhou, Tanmoy Bhattacharya, Duong Tran, Tuck Sing Terence Siew and Ashwin M. Khambadkone, "Composite Energy Storage System Involving Battery and Ultracapacitor with Dynamic Energy Management in Microgrid Applications," IEEE Transactions on Power Electronics, Vol. 26, No. 3, March 2011.
7. Sharad W. Mohod and Mohan V. Aware, "Micro Wind Power Generator with Battery Energy Storage for Critical Load," IEEE Systems Journal, Vol. 6, No. 1, pp. 118-125, March 2012.
8. Perna Gaur and Sunita Singh, "Investigations on Issues in Microgrids," Journal of Clean Energy Technologies, Vol. 5, No. 1, January 2017.
9. J. C. Vasquez, R. A. Mastromauro, J. M. Guerrero, and M. Liserre, "Voltage Support Provided by a Droop-Controlled Multifunctional Inverter," IEEE Trans. Ind. Electron., Vol. 56, pp. 4510–4519, 2009.
10. L. D. Watson and J. W. Kimball, "Frequency Regulation of a Microgrid using Solar Power," in Proc. 2011 IEEE APEC, pp. 321–326.
11. L. Xu, Z. Miao, and L. Fan, "Coordinated Control of a Solar Battery System in a Microgrid," in Proc. 2012 IEEE/PES Transm. Distrib. Conf. Expo. (T&D), pp. 1–7.
12. Joe-Air Jiang, Tsong-Liang Huang, "Maximum Power Tracking for Photovoltaic Power Systems," Tamkang Journal of Science and Engineering, Vol. 8, No. 2, pp. 147-153, 2005.
13. Marcelo Gradella Villalva, Jonas Rafael Gazoli, and Ernesto Ruppert Filho, "Comprehensive Approach to Modeling and Simulation of Photovoltaic Arrays," IEEE Transaction on Power Electronics., Vol. 24, No. 5, pp. 1198–1208, May 2009.
14. P. F. Ribeiro, B. K. Johnson, M. L. Crow, A. Arsoy, and Y. Liu, "Energy Storage System for Advance Power Applications," Proc. IEEE, Vol. 89, No. 12, pp. 1744–1756, Dec. 2001.
15. O. Tremblay and L. A. Dessaint, "Experimental Validation of a Battery Dynamics Model for EV Applications," in world Electric Vehicle J., Vol. 3, 2009.
16. B. Singh, S. S. Murthy, and S. Gupta, "Analysis and Design of STATCOM-Based Voltage Regulator for Self-Excited Induction Generator," IEEE Transaction on Energy Conversion, Vol. 19, No. 4, pp. 783–791, December 2004.
17. Sarina Adhikari and Fangxing Li, "Coordinated V-f and P-Q Control of Solar Photovoltaic Generators With MPPT and Battery Storage in Microgrids," IEEE Transactions on Smart Grid, Vol. 5, No. 3, May 2014.

18. Sarina Adhikari, Fangxing Li and Huijuan Li, "P-Q and P-V Control of Photovoltaic Generators in Distribution Systems", IEEE Transactions on Smart Grid, 2015.
19. Yan Xu, Huijuan Li. D. Tom Rizy, Fangxing Li, John D. Kueck, "Instantaneous Active and Nonactive Power Control of Distributed Energy Resources with a Current Limiter," in IEEE conference, pp. 3855-3861, 2010.



Shridhar S. Khule received the B.E. degree in Electrical Engineering from AISSMS College of Engineering, Pune, Maharashtra (India) in 2000 and Master of Engineering from Walchand College of Engineering, Sangli, Maharashtra (India) in 2007. Currently, he is pursuing the Ph.D. degree from Prof. Ram Meghe Institute of Technology and Research, Badnera, Amravati, Maharashtra (India). He worked as a Assistant Professor in Sir Visvesvaraya Institute of Technology, Nashik, Maharashtra (India) from 2002 to 2011. Since 2011, he has been an Associate Professor with the Department of Electrical Engineering, Matoshri College of Engineering & Research Center, Nashik, India.



Dr. Sharad W. Mohod received the B.E. and M.E. degrees in Electrical Engineering from Government College of Engineering, Aurangabad, India in 1988 and 1992, respectively and the Ph. D. degree from Visvesvaraya National Institute of Technology, Nagpur, India in 2012. He has worked with Garware Polyester Ltd., Aurangabad, from 1988-1991. In 1991, he joins College of Engineering Badnera, Amravati, and from 2011, he is working as a Professor in Department of Electronics and Telecommunication Engineering, Prof. Ram Meghe Institute of Technology & Research, Badnera, Amravati, India. Currently he is a Chairman of Institution of Engineer (India), Amravati Local Centre, Fellow of FIE, MIE (I), IETE, LMISTE and Chartered Engineer. His research interests include power quality, renewable energy sources, and power electronic applications to power systems.